

VALIDATION OF CONSTRAINT BASED METHODOLOGY IN STRUCTURAL INTEGRITY – VOCALIST: ANALYTICAL PROGRAMME

Elisabeth Keim, Michael Ludwig,
Framatome ANP,
Germany

Richard Bass, Wallace McAfee,
Sean Yin, Paul Williams, ORNL,
USA

Yves Wadier, EDF,
France

Philippe Gilles, Framatome ANP, France

David Lidbury, Andrew Sherry,
Serco Assurance, UK

Heikki Keinänen, Kim Wallin,
VTT, Finland

Stéphane Marie, Stéphane
Chapuliot, CEA,
France

Ulrich Eisele, MPA Stuttgart,
Germany

ABSTRACT

The aim of the EC project VOCALIST (Validation of Constraint-Based Assessment Methodology in Structural Integrity) is to develop and validate innovative procedures for assessing the level of, and possible changes to, constraint-based safety margins in ageing nuclear pressure boundary components. An iterative process of experiment and analysis will address this overall objective.

The analytical investigations within VOCALIST cover all three ferritic materials used in the experimental program. Two of the three materials are investigated in the brittle to transition regime and the third material will be tested in the ductile regime.

The main effort is to predict the results of the large-scale tests in terms of constraint effects. All participants use constraint based methods, which are in a first step calibrated to the behaviour of well-known specimens and then applied to the features or the large scale tests of each material. In this contribution the progress of the analytical program of VOCALIST since last year will be reported. The analyses of the specimens and components under investigation are highlighted with respect to modelling aspects and the first results are presented.

INTRODUCTION

The VOCALIST project [1] is divided into six work-packages. The analysis work-package deals mainly with design and prediction of the features tests (small or medium-scale tests) and benchmark tests (large-scale tests). The main work during the first period of the project was the selection of appropriate pre-existing benchmark tests and the design of the

features tests [2]. In this second period more a lot of work was performed to calibrate the constraint-based local models. Three materials were chosen as being representative for the purpose of the project, but appropriate benchmark tests were not available in every case. However, it turned out that the missing tests could be conducted with support from outside the framework of VOCALIST under the auspices of the European Network NESC.

MATERIALS

Three materials are under investigation:

Material A: forged, quenched and tempered large ring segment of the ferritic steel DIN 22 NiMoCr 3 7, which corresponds to ASTM A508 Grade 3 Cl 1. Properties representative of an RPV at start of life.

Material D A533B ferritic steel (HSST Plate 14) heat treated to achieve an elevated yield strength (range 620-655 MPa at RT) approximating that for a typical radiation sensitive RPV steel irradiated to a fluence of 1.5×10^{19} n/cm² ($E_n > 1\text{MeV}$).

Material P: French Tu52b ferritic steel for pipes. The properties correspond to begin of life conditions.

The specimens and structures that are analysed will be described in detail in the following sections. For material A a modified compact tension specimen (features test) and a cruciform bend specimen (benchmark test) are investigated.

ANALYTICAL APPROACHES AND RESULTS

EDF Energy Approach [3]

The application of the energy approach of EPFM to the analysis of the constraint effect observed on characterisation tests on SENB specimens will be described.

The energy approach has been developed at EDF – R&D for cleavage fracture as well as for ductile tearing [4]. In the case of cleavage fracture we start from Francfort and Marigo elastic fracture theory [5], based on a minimum energy principle, which generalises the Griffith theory in order to predict initiation or discontinuous propagation of cracks. A parameter “Gp” can then be defined as an energy release rate in the context of the incremental theory of plasticity [6]. It has the great advantage of being not mesh dependent. It can be used to analyse all situations of cleavage fracture where the J-approach is not valid, such as problems with unloading [7], non proportional loading, residual stresses, or problems related to the shallow crack effect [8].

In the context of VOCALIST, different tests have been performed on 25 mm thick SENB specimens made of an high toughness ferritic RPV steel (Material A) and containing deep ($a/w = 0.5$) and shallow ($a/w = 0.1$) cracks. The tests were performed at different temperatures: -110°C , -90°C , -60°C , -40°C . In this study we have only considered the two extreme temperature values: -110°C and -40°C . The mean toughness value is equal to $72.\text{MPa.m}^{1/2}$ at -110°C and to $225.\text{MPa.m}^{1/2}$ at -40°C . The numerical analysis was performed at EDF-R&D with the Code-Aster, the finite element code of EDF, to analyse these tests. Three geometries were analysed: two related to the deep and shallow crack SENB specimens and one related to a CT specimen in order to identify the critical value of the parameter Gp.

We have considered a 2D problem assuming plane strain hypothesis. The constitutive law is elastoplastic with an isotropic hardening. The crack is represented as a very thin notch, “r” being the radius of the circle defining the crack tip. We define the shallow crack effect “SCE” as the value of: K_{jc} (predicted on the SENB specimen) / K_{jc} (identified on the CT specimen). After having identified the critical value of Gp using the CT specimen, the toughness of the SENB specimens was predicted and following results were obtained:

K_{jc} (at -110°C) = $75.\text{MPa.m}^{1/2}$, for the deep crack specimen, (72. for the CT), giving: SCE = 1.04

K_{jc} (at -110°C) = $142.\text{MPa.m}^{1/2}$. for the shallow crack specimen, (72. for the CT), giving : SCE = 1.97

K_{jc} (at -40°C) = $297.\text{MPa.m}^{1/2}$, for the deep crack specimen, (225. for the CT), giving: SCE = 1.32

K_{jc} (at -40°C) = $425.\text{MPa.m}^{1/2}$. for the shallow crack specimen, (225. for the CT), giving : SCE = 1.89

The shallow crack effect is clearly obtained between the CT specimen and the shallow crack SENB specimen. At -110°C , there is no geometrical effect between the CT and the deep crack SENB specimen, but at -40°C , some geometrical effect can be observed. At the present time we cannot validate these results by comparison to experimental ones, which are not yet available. A correlation is obtained between the parameter Gp and the triaxiality parameter calculated along the area corresponding to the notch propagation. Finally, a parametric study is performed in order to estimate the influence of the stress/strain curve and the influence of the choice of the value of “r”. This study confirms the validity of the first prediction.

VTT Unit Cell Model

In order to determine valid Tstress and Q-parameter values to be applied in fracture toughness transferability analyses, finite element analyses of a 'unit cell model' and the cruciform bend specimen have been performed. A unit cell model, a bend block with a crack length to specimen width ratio of 0.1, was used to parametrically study the means to characterize biaxial loading effects to fracture toughness transferability by using the T-stress and Q constraint parameters. This model implied a constraint increase for T-stress arising from biaxial loading to be of the order of 0.16 in terms of T/σ . The value is reasonable if applied to constraint evaluation of the cruciform specimen test results. However, some conflicting results have been presented for the T-stress in terms of loading biaxiality dependency, i.e. finite element results of Oak Ridge have implied that the constraint increase from biaxial loading would not be as large in the cruciform specimens. The T-stress analysis results for the biaxial bend specimens utilizing the 'unit cell' computed biaxial Tstress values are presented in Figure 1. In order to solve the difference in results between these two different models, it was decided to also investigate the cruciform specimen under 1 axial and 2 axial bending, respectively. The finite element models are presented below in Figures 2 and 3. These analyses are underway and both linear-elastic and elastic-plastic analyses will be performed to determine the T-stress and Q values and compare to those presented by Oak Ridge.

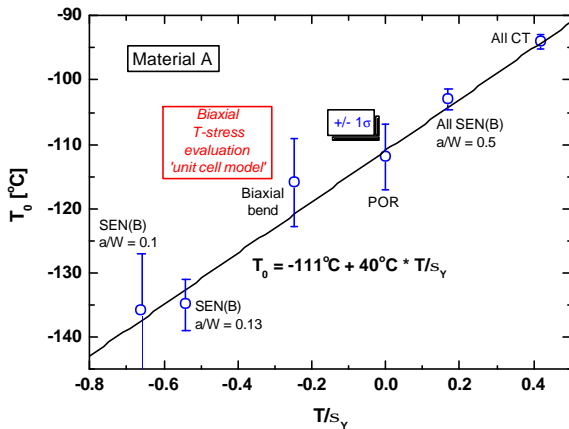


Figure 1. Dependency of reference temperature on T-stress, biaxial bend results analysed using a T-stress solution for a 'unit cell' model under biaxial loading

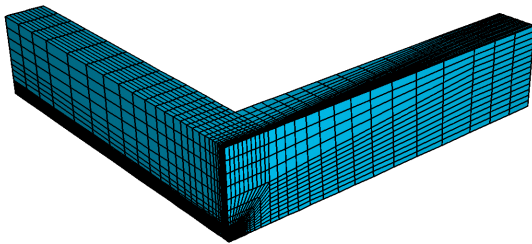


Figure 2. Mesh of the cruciform specimen

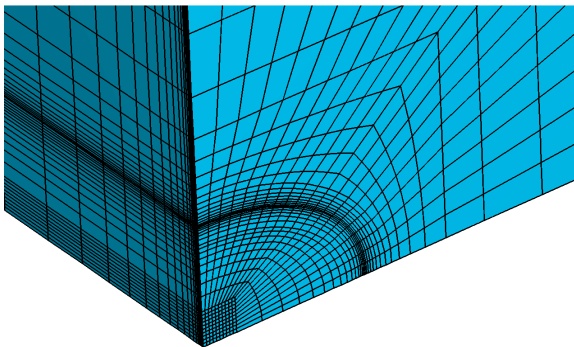


Figure 3. Near crack tip mesh of the cruciform specimen

CEA Approach

CEA is involved in the analyses of cracked pipe tests: The modelling of the two tests is planned, using conventional approach (based on J - Δa curve), local approach (Rousselier model) and energetic approach (Ji-Gfr approach).

The J - Δa curve has been determined from CT test performed in the frame of the experimental work. Parameters for the energetic approach are already available for the material P. The calibration work is then focused on the Rousselier model. For this task, required material data are experimental results of CT and round notched bar tests.

The models parameters calibration should be presented during next PMB meeting. FE modelling of the pipe tests should start during this summer, but it depends on the time scale of the second features test. At least, the calculation for the first pipe test should be ready for the futur PMB meeting.

ORNL Cleavage fracture prediction of shallow-flaw cruciform beams using a Weibull stress model

As part of the VOCALIST project, a Weibull stress statistical fracture model for Material A (EURO RPV Steel) using the G-R-D calibration scheme [9] has been applied to fracture analyses of the Euro steel biaxial cruciform and uniaxial bend-bar specimens under low- and high-constraint conditions at the crack front.

Fracture Experiments

In the testing program, seven cruciform beams were tested to failure in cleavage fracture under biaxial bending. Six beams were tested under a constant 1:1 equibiaxial loading ratio, and one with 0.87:1. Most beams were tested at -60 °C except the first two at -50 °C. The toughness data (K_{Jc}) were estimated using eta-factors with CMOD data.

Calibration Procedures

1. The *Master Curve* Weibull statistical model was used to stochastically simulate two sets of fracture toughness data with different crack configurations (shallow flaw with $a/w = 0.1$, and deep flaw with $a/w = 0.5$). Based on an evaluation of all available EURO material data, Professor K. Wallin, VTT, Finland, recommended that the following material reference temperatures T_0 be used in the analysis: $a/w = 0.1$, $T_0 = -137$ °C; $a/w = 0.5$, $T_0 = -105$ °C. For this special material, simulated J -integral data at -60 °C for 1T SE(B) deep flaw specimen ranges 26~403 kJ/m², and 73~1179 kJ/m² for shallow flaw specimens, shown in Figure 4.
2. Detailed, 3D sharp-tip and blunt-tip finite-element models were developed for the two SE(B) specimens, and the plane-strain, SSY Modified Boundary Layer

model was also used for the calibration of Weibull stress parameters, shown in Figure 5.

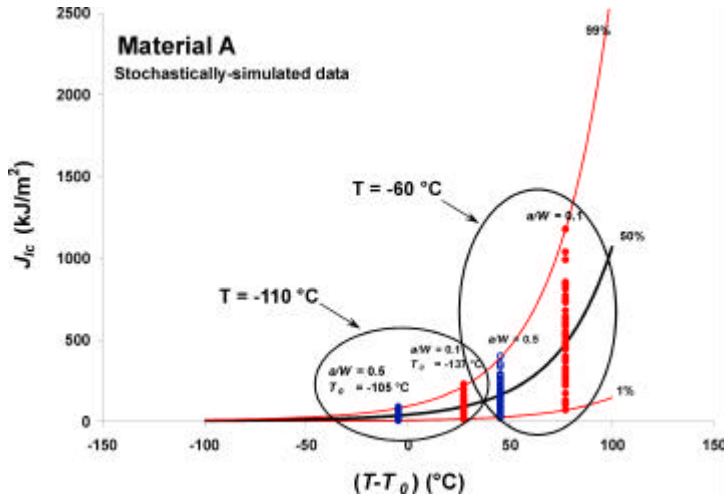


Fig. 4. Stochastically-generated J_{IC} fracture toughness data for shallow-flaw ($a/W = 0.1$) and deep-flaw ($a/W = 0.5$) SE(B) 1T specimens for two test temperatures, $-110\text{ }^{\circ}\text{C}$ and $-60\text{ }^{\circ}\text{C}$.

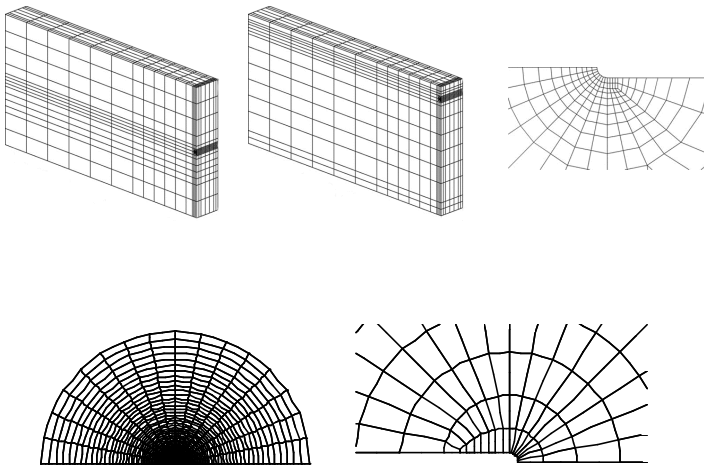


Fig. 5. Quarter-finite-element models of SE(B) 1T specimens: (a) deep-flaw specimen, $a/W = 0.5$, (b) shallow-flaw specimen, $a/W = 0.1$, (c) detail of finite-root tip meshing for blunt-tip models, (d) MBL SSY model, and (e) close-up of MBL SSY finite-root blunt crack tip.

Sharp-tip models were used to calibrate Load vs. J -integral information of the material. Blunt-tip models were utilized to

generate crack-tip stress and strain fields as input for Weibull stress calculations. The shallow-flaw and deep-flaw finite element models were built using Material A properties at $T = -60\text{ }^{\circ}\text{C}$. Tensile effective stress vs effective plastic strain curves for the material are shown in Figure 6 for three temperatures.

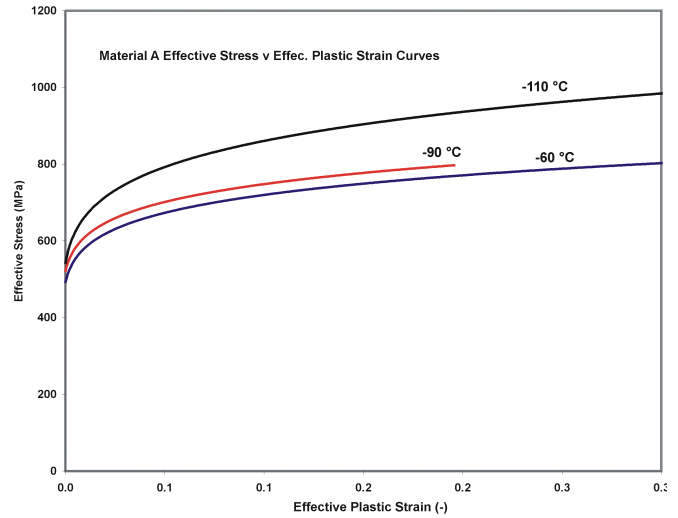


Fig. 6. Effective stress vs effective plastic strain for Material A (Euro Steel) at three temperatures, $-60\text{ }^{\circ}\text{C}$, $-90\text{ }^{\circ}\text{C}$, and $-110\text{ }^{\circ}\text{C}$.

In the ORNL approach, the calibration of the Weibull stress parameters is based on hydrostatic stress to capture the constraint effect due to the biaxial loading. Because of the wide scatter of simulated fracture toughness data, substantially high loadings have to be applied to the shallow-flaw and deep-flaw models in order to cover the simulated “experimental” data in the Weibull stress calculation. Therefore, the models deformed with high plastic deformation, which may not be realistic in the experiments, shown in Figure 7. Inside the modified WSTRESS code, the fracture process zone near the crack-tip is defined as the volume including all of the material elements satisfying the condition $s_{eff} \geq I s_0$, where s_0 is the yield stress and s_{eff} is the Mises effective stress. A well-defined fracture process zone could not be achieved in models by choosing the default cut parameter $I = 0.9$. It was observed that the calibration is very sensitive to the choice of the cut parameter. To get a reasonable region, a cut parameter $I = 1.2$ was used in the calibration, shown in Figure 8.

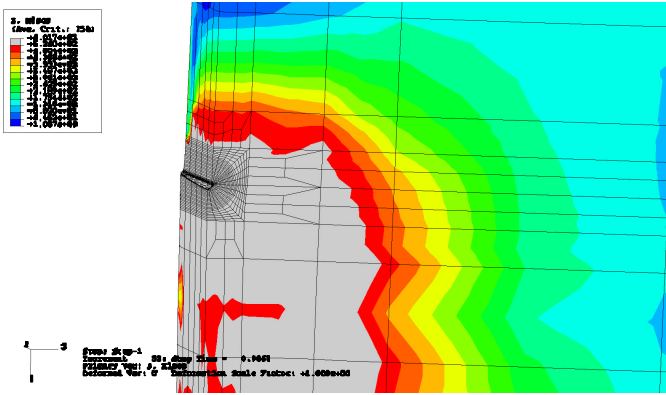


Fig. 7. Deformed blunt-tip deep flaw model with cut parameter $l=1.0$ where the gray region depicts the material inside the fracture process zone as defined by $s_{eff} \geq l s_0$.

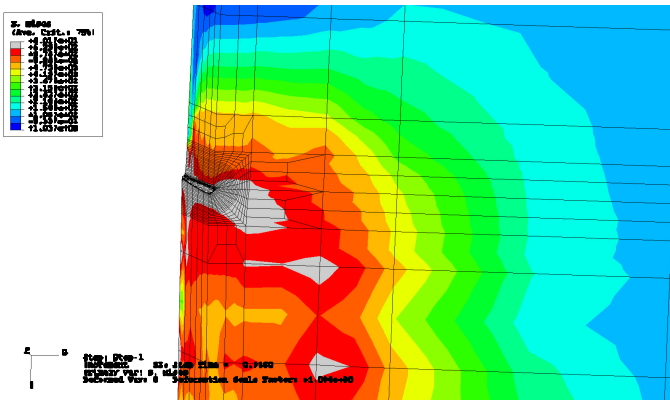


Fig. 8. Deformed blunt-tip deep flaw model with cut parameter $l=1.2$.

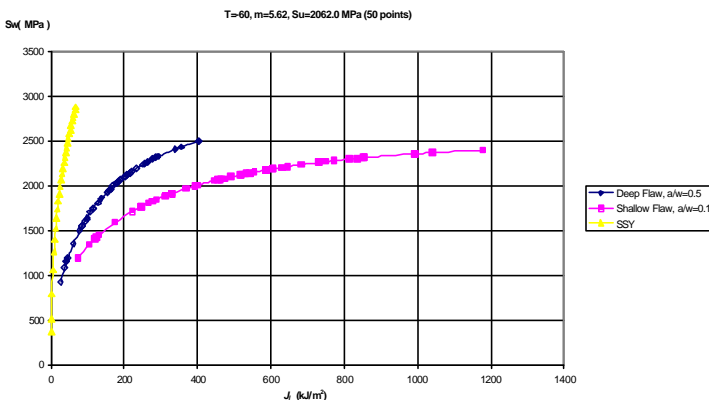


Fig. 9. Weibull stress as a function of J -integral for converged calibration: $T = -60$ °C, $m = 5.62$, $s_u = 2062$ MPa, 50 data points.

The Weibull stress model was calibrated (based on uniaxial SE(B) 1T finite-element models and stochastically-generated fracture toughness data only) with a Weibull shape parameter of $m = 5.62$, and a Weibull scale factor of $s_u = 2062.0 \text{ MPa}$, as shown in Figure 9. These Weibull model parameters were used to perform fracture assessments of the EURO cruciform 4T beams tests conducted at ORNL under biaxial loading.

Prediction of cleavage fracture in cruciform beams with shallow flaw

The calibrated three-parameter Weibull stress model was applied to predict the cumulative failure probability for cleavage fracture of the tested EURO cruciform 4T specimens. A $1/4$ three-dimensional model (20,451 nodes and 4,301 20-node isotropic brick elements), shown in Figure 10, was developed for local crack-tip stress and deformation field analyses.

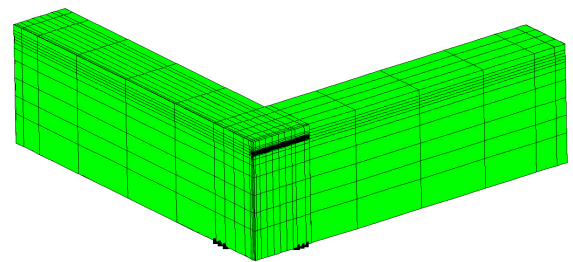


Fig. 10. Finite element $1/4$ model of cruciform 4T beam specimen ($a/w = 0.1$).

After comparing the overall predicted Load-CMOD (Crack Mouth Open Displacement) response with experimental records, the material properties of the finite-element model were slightly modified. These modifications were carried out to match both the elastic and the plastic deformation compliance of the model with the experimental LOAD vs CMOD data. The numerical and experimental responses are shown in Figure 11. The elastic modulus of the material was reduced from 213240 MPa to 163406 MPa. The 0.2% offset yield strength was experimentally determined to be 488 MPa at the test temperature of -60 °C. Previous uniaxial tensile data provided by Framatome-ANP, Germany gave a value of 524 MPa at this temperature. The effective stress vs effective plastic strain curve was modified accordingly.

Figure 12 compares the predicted failure probabilities using the Weibull stress model ($m = 5.62$, $s_u = 2062.0 \text{ MPa}$) with the estimated probabilities (based on median-rank order statistics) for the measured J -integrals. Since the crack front length of the beams (4T) equals $4 \times$ that of the SE(B) specimens (1T), the experimental J -integrals data were scaled to 1T data with equations:

$$K_{Jc(1T)} = K_{Min} + \left[K_{Jc(x)} - K_{Min} \left(\frac{B_x}{B_{1T}} \right)^{1/4} \right] MPa\sqrt{m}$$

where $K_{min} = 20MPa\sqrt{m}$ for common ferritic steels, B_{1T} represents the 1T specimen size (25.4mm) and B_x is the crack length of the 4T cruciform beams 101.6 mm, and $K_{Jc} = \sqrt{EJ_{IC} / (1 - u^2)}$.

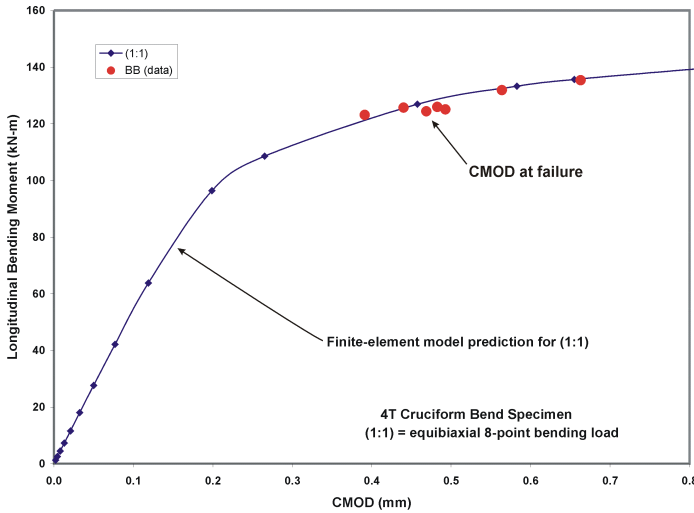


Fig. 11. Comparison of finite-element model prediction (using modified property data) of elastic and plastic compliance of 4T cruciform bend specimen under equibiaxial (1:1) loading with CMOD at failure data from VOCALIST cruciform bend tests at -60°C.

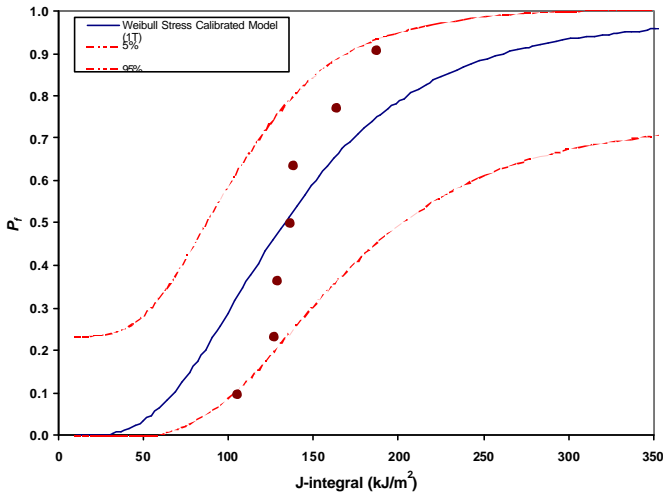


Fig.12. Comparison of predicted cumulative failure probability of cruciform beams under biaxial loading with experimental data.

The model predictions capture the measured toughness distribution. Also the 90% confidence limits for the estimates of rank probability for the experimental data are shown in Figure 12. It indicates that all order rank probabilities of the experimental data lie within the 90% confidence limits. These 90% confidence limits were calculated based on the procedures provided in ref [10].

Framatome ANP Cleavage fracture prediction for fracture mechanic specimens with straight and semi-elliptical crack front using a three parameter Weibull stress model

As part of the VOCALIST project and continuation of the work presented in [2] a three parameter Weibull model is applied to predict the cleavage fracture probability and transition temperature T_0 shift for fracture mechanic specimens with different size, geometry and constraint conditions.

Fracture toughness test data

For calibration and testing the Weibull cleavage fracture model different data sets are available. In our case, deep and shallow flaw 10x10mm² PCCV specimens, tested within the VOCALIST project, are used for calibration and determination of the Weibull parameters. The shallow flaw test data were separated into two sets of a/W ratios, one set with a/W=0.09-0.12 and the other set with a/W=0.12-0.145. The first data set consists of 7 test results with a $T_0 = -146^\circ C$. The second set, which was actually used in the calculations as low constraint data, contains 20 results with a $T_0 = -140^\circ C$. As deep flaw high constraint data 10 PCCV 10x10mm² specimens with $T_0 = -122^\circ C$ and a/W=0.5 are used to calculate the Weibull parameters. To analyse the applicability of the Weibull model to the various specimen sizes, load-types (bending and tension) and geometries (CT, SENB, POR specimens) additional test data are used. Within the VOCALIST-Project test data for deep and shallow flaw SENB 25x25mm² specimens are produced, with $T_{0-shallow} = -133^\circ C$ and $T_{0-deep} = -118^\circ C$ as well as data for the feature tests, which are CT specimens containing semi-elliptical surface flaws, called POR specimens. In addition data from CT tests with different W ratios are used to understand the dependency of the Weibull model with varying thickness. Table 1 shows the test data of all specimens used for the Weibull model calibration and prediction.

	T_0 °C	$K_{Jc} [med]$ MPa $\sqrt{m}^{0.5}$
PCCV 10X10mm ² a/W=0.1	-146	233
PCCV 10X10mm ² a/W=0.14	-140	211
PCCV 10X10mm ² a/W=0.5	-122	158
SENB 25X25mm ² a/W=0.1	-133	201
SENB 25X25mm ² a/W=0.5	-118	138
POR (feature test, B=50, W=100)	-111	134
2TCT W=100 a/W=0.5	-85	94
47CT W=200 a/W=0.5	-77	85

Table 1. Test data used for calibration and checking the Weibull model

Weibull calibration with high and low constraint toughness data

Gao et al [9] proposed a method for the calculation and prediction of the transition temperature T_0 for structures with varying constraint conditions. He suggested to calculate the Weibull parameters with two sets of fracture toughness data with different crack tip constraint. All large scale yielding (LSY) toughness data are mapped back into a small scale yielding space (SSY). The results are SSY data for both sets of LSY data. After calibration the data show the same statistical behavior in the SSY space, described by the Weibull parameters m , σ_U , σ_{W-min} and β . In the presented calibration the PCCV data with $a/W=0.5$ and $a/W=0.14$ provides the database for the calibration. The Weibull stress is calculated by the integration over a fracture process zone which includes all integration points with maximum principal stress values higher than the yield stress at test temperature. Figure 11 depicts the calibrated LSY and SSY data for both specimen configurations and the Weibull stress vs. J-Integral values for the SSY solution.

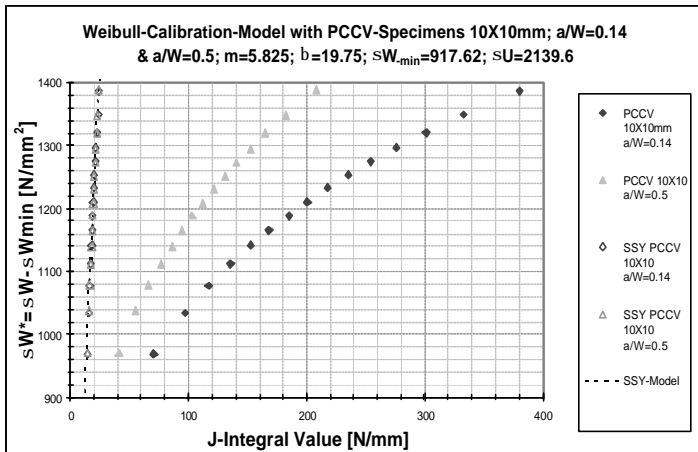


Fig. 13. Weibull stress vs. J-Integral for converged calibration

The calibrated Weibull parameters describe now the difference in fracture toughness for the two data sets with different crack tip constraint.

Prediction of fracture toughness values for specimens with different load-type and geometrical shape

The Weibull parameters calculated in the calibration should now be used to predict the fracture toughness data for the different specimens given in Table 1. For all specimens detailed three dimensional finite element calculations were performed to calculate the σ_W -J history. Figure 12 shows the σ_W -J data for all specimens used in this analysis. The J-Values are normalized by β ($\beta=19.75$ N/mm) which corresponds to

the J value at σ_U in the SSY stress space. The x-axis shows the ratio of σ_W^*/σ_U^* ($\sigma_W^*=\sigma_W-\sigma_{W-min}$; $\sigma_U^*=\sigma_U-\sigma_{W-min}$). The J-Values at 50% failure probability for the different specimens follow from σ_W^*/σ_U^* at $\sigma_W^*/\sigma_U^*=0.93902$ ($\sigma_{W-min}=917,6$ N/mm², $\sigma_U=2139,6$ N/mm²). To compare the σ_W values of each specimen with the solution of the calibration, all σ_W stresses are scaled relatively to the fracture process zone of the PCCV 10x10mm² specimens.

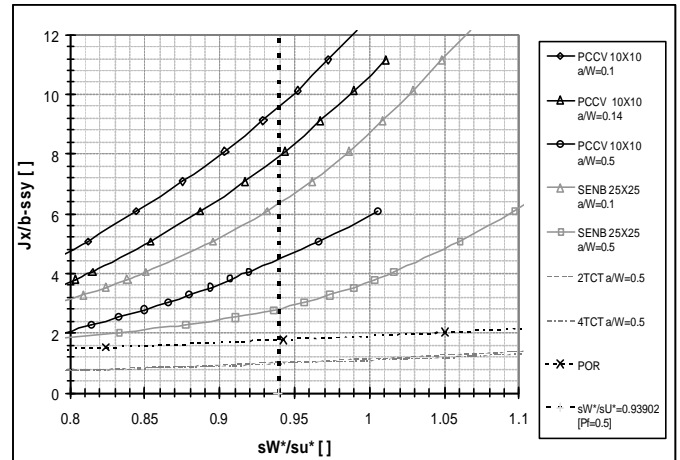


Fig. 14. Normalized J-Integral and Weibull stresses (J/b_{-ssy} vs. sW^*/sU^*)

Figure 13 shows all the fracture toughness values K_{Jcmed} for all specimens with 5% and 95% tolerance bounds and the predicted $K_{Jcmed-prediction}$ calculated with the cleavage fracture model. The PCCV 10x10mm² values used for the calibration and the predicted toughness data for the SENB 25x25mm² specimens agree well with the test results. The prediction of the POR and CT-Specimens show a difference in K_{Jcmed} compared to the test values.

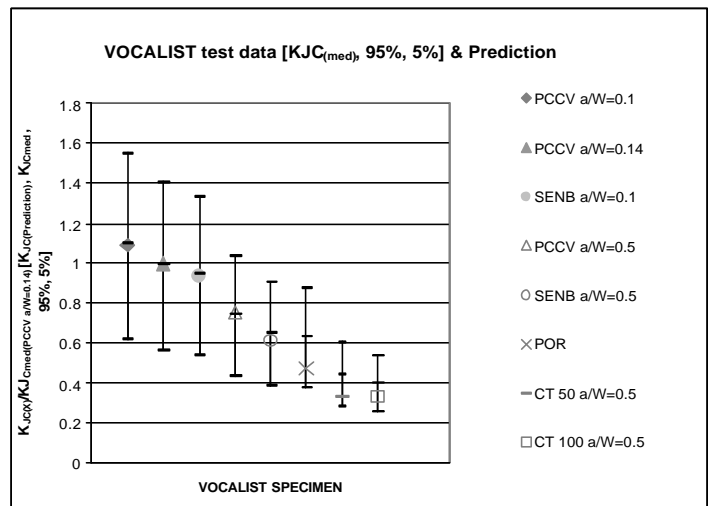


Fig. 15. Test results and prediction

SUMMARY

The presented results summarize the progress in the analytical part of the project. Various methods are applied to predict constraint effects on fracture toughness in the transition regime and to account for the different high and low constraint specimen results. The next step will be finish all calculations for all three materials and to draw conclusions about the applied methods.

REFERENCES

[1] Lidbury D., et al: « Validation Of Constraint Based Methodology in Structural Integrity – VOCALIST” Contribution to ASME PVP, 2002.

[2] Keim E., et al: “VALIDATION OF CONSTRAINT BASED METHODOLOGY IN STRUCTURAL INTEGRITY – VOCALIST: Analytical programme, PVP 2002, Vancouver

[3] Y. Wadier, M. Bonnamy, “PROGRAMME VOCALIST: THE ENERGY APPROACH OF ELASTOPLASTIC FRACTURE MECHANICS APPLIED TO THE ANALYSIS OF THE CONSTRAINT EFFECT”, to be published in the proceedings of the PVP 2003, Cleveland

[4] Wadier Y., Debruyne G., « New energetic parameters for cleavage fracture and ductile tearing: application to the analysis of a subclad flaw located in a pressure vessel of a PWR », PVP 2000, Seattle.

[5] Francfort G., Marigo J.J. : « Revisiting brittle fracture as an energy minimization problem », J. Mech. Phys. Solids, 1998.

[6] Lorentz E., Wadier Y., Debruyne G. (2000), « Mécanique de la rupture en présence de plasticité : définition d’un taux de restitution d’énergie ». C.R.A.S. t. 328, série IIb.

[7] Wadier Y., Lorentz E., « The energetic approach of elastic-plastic fracture mechanics applied to the problem of unloading » SMiRT 16 - 2001, Washington.

[8] Wadier Y., Lorentz E., « New considerations and results on crack separation energy rates in elastic-plastic fracture mechanics », ICF10, December 2001, Honolulu.

[9] X. Gao, C. Ruggieri, and R. H. Dodds, Jr., “Calibration of Weibull Stress Parameters using Fracture Toughness Data,” *International Journal of Fracture* 92, (1998) 175-200.

[10] X. Gao, R. H. Dodds, R. L., Tregoning, J. A. Joyce, and R. E. Link, “A Weibull Stress Model to Predict Cleavage Fracture in Plates Containing Surface Cracks,” *Fatigue Fract. Engng. Mater. Struct.* **22**, (1999) 481-493.